STATISTICS, OPTIMIZATION AND INFORMATION COMPUTING
Stat., Optim. Inf. Comput., Vol. **14**, December 2025, pp 3633–3650.
Published online in International Academic Press (www.IAPress.org)

Examining the One-Step Implicit Scheme with Fuzzy Derivatives to Investigate the Uncertainty Behavior of Several First-Order Real-Life Models

Kashif Hussain[1], Ala Amourah[2,3,*], Jamal Salah[4,*], Ali Jameel[2], Emad A. Az-Zo'bi[5], Mohammad A. Tashtoush[6,2], Muhammad Zaini Ahmad[1] and Tala Sasa [7]

[1] *Institution of Engineering Mathematics, Universiti Malaysia Perlis*
[2] *Mathematics Education Program, Faculty of Education and Arts, Sohar University, Sohar 311, Oman*
[3] *Jadara Research Center, Jadara University, Irbid, Jordan*
[4] *College of Applied and Health Sciences, A'Sharqiyah University, Post Box No. 42, Post Code No. 400 Ibra, Sultanate of Oman*
[5] *Mathematics and Statistics Department, Faculty of Science, Mutah University, AL-Karak, Jordan*
[6] *Department of Basic Science, AL-Huson University College, AL-Balqa Applied University, Salt 19117, Jordan*
[7] *Department of Mathematics, Faculty of Science, Applied Science Private University, Amman, Jordan*

Abstract Differential equations (DE) are useful for representing a variety of concepts and circumstances. However, when considering the initial or boundary conditions for these DEs models, the usage of fuzzy numbers is more realistic and flexible since the parameters can fluctuate within a certain range. Such scenarios are referred to as unexpected conditions and introduce the idea of uncertainty. These issues are dealt with using fuzzy derivatives and fuzzy differential equations (FDEs). When there is no precise solution to FDEs, numerical methods are utilized to obtain an approximation solution. In this study, the One-step Implicit Scheme (OIS) with a higher fuzzy derivative is extensively used to discover optimum solutions to first-order FDEs with improved accuracy in terms of absolute accuracy. We evaluated the method competency by investigating first-order real-life models with fuzzy initial value problems (FIVPs) in the Hukuhaa derivative category. The principles of fuzzy sets theory and fuzzy calculus were utilized to give a new generic fuzzification formulation of the OIS approach with the Taylor series, followed by a detailed fuzzy analysis of the existing problems. OIS is acknowledged as a practical, convergent, and zero-stable approach with absolute stability region for solving linear and nonlinear fuzzy models, as well as a useful methodology for properly managing the convergence of approximate solutions. The capabilities of the developed scheme are proved by providing approximate solutions to real-life problems. The numerical findings demonstrate that OIS is a viable and transformative approach to solving first-order linear and nonlinear FIVPs. The results provide a concise, efficient, and user-friendly approach to dealing with larger FDEs.

Keywords First-Oder, One-Step Scheme, Fuzzy Derivative, Zero-Stability, Real-Life Models.

AMS 2010 subject classifications 97N40, 34XX

DOI: 10.19139/soic-2310-5070-2250

1. Introduction

Differential equations DEs are widely used in many domains because they can express the connection between a quantity and its rate of change. Some typical applications of differential equations are physics, computer science, engineering, biology, economics, finance, chemistry, environmental science, medicine, and control systems [1].

The uncertain behavior of differential equations refers to circumstances in which little modifications or uncertainties in the initial conditions or parameters of a differential equation can result in drastically different results

*Correspondence to: Ala Amourah (Email: AAmourah@su.edu.om). Mathematics Education Program, Faculty of Education and Arts, Sohar University, Sohar 311, Oman

ISSN 2310-5070 (online) ISSN 2311-004X (print)

over time. This sensitivity to beginning circumstances is typical of various nonlinear differential equations and is frequently connected with chaotic behavior. Chaotic behavior may occur in a variety of physical, biological, and ecological systems and has been found in specific types of differential equation, including the well-known Lorenz system. Understanding and evaluating the unpredictable behavior of these systems requires advanced mathematical techniques and numerical simulations. Differential equations have many applications, including engineering, biology, chemistry, electronics, and physics. Unfortunately, unanticipated events may arise that introduce the concept of uncertainty and the use of FDEs to address these issues. This chapter contains real-life problems such as liquid tank system thermal system nuclear decay model electrical circuit charging and discharging capacitor model simple damping pendulum mass vibrate system and SIR model. These considered differential equationdels are in fuzzy form with uncertain bbbbehavior andndndnd are numerically solved by the constructed block methods with the presence of two hderivativeeee terms. Zadeh and Chang [2] introduced the notion of fuzzy derivatives in 1972. Puri and Ralescu [3], Seikkala [4], and Bede and Gal [5] developed the three primary definitions for the differential of the fuzzy function. Hukuhara derivative, Seikkala derivative, and generalized derivative. Due to the difficulty in getting accurate solutions to fuzzy ordinary differential equations (FDEs), numerical methods are used to solve them. When applying the numerical methods to FDEs, researchers use the crisp function of ODEs with the parametric form of fuzzy numbers as an initial condition. Thus, the initial condition consists of the lower and upper bounds of fuzzy numbers.

Numerical solutions of first-order FDEs with FIVPs using the Euler method were introduced by Ma et al. [6]. Subsequently, modifications to the conventional Euler method have been explored, such as Shokri [7] proposing two approaches based on the slandered Euler method and the extension of Zadeh. Similarly, the generalized Euler approximation method with order two was used [8, 9, 10]. They developed two forms of this numerical method; first, minimum-maximum and second, average Euler method. They solved first-order linear and nonlinear FIVPs using triangular and trapezoidal fuzzy numbers, and the accuracy in terms of error was compared with the conventional Euler method. Sevindir and Cetinkaya [11] and Ahmady et al. [12] adopted the classical Euler method, Homotopy analysis method (HAM), and Adomian decomposition method to solve the linear fuzzy Cauchy problem. The advantages of the Euler method include being simple, direct, and it can be used for nonlinear FIVPs. However, the disadvantages of this method include being less accurate, numerically unstable, and approximation error being proportional to the step size h [13]. Hence, a good approximation is obtained with a very small h. This requires a large number of time discretization leading to a large computation time.

Another class of methods adopted for first-order ODEs is the predictor-corrector method. Allahviranloo et al. [14] used the Adams-Bashforth four-step and Adams-Moulton three-step methods to solve linear fuzzy FDEs. In the same way, [15, 16] developed a hybrid multistep method (predictor-corrector) for first-order linear examples of FIVPs. They developed these hybrid methods to enhance the accuracy and computing speed of the numerical solutions of FIVPs. Despite the modifications, the accuracy in terms of absolute error is still low. The trapezoidal method was suggested by Ivaz et al. [17] for the numerical solution of the FIVPs using fuzzy triangular numbers as initial conditions for the crisp ODE. In other studies, [18, 19] used the Simpson method for the solution of the FIVPs.

Abbasbandy et al. [20] first developed the RK method of order two to solve FDEs numerically, while Kanagarajan and Sambath [21] developed and applied the third-order RK method. Jameel et al. [22] developed the fifth-order RK method using the trapezoidal and fuzzy triangular numbers as an initial condition to solve first-order linear FIVPs. Parandin [23] and Nirmala et al. [24] developed a second-order RK method for FDEs under the generalized differentiability concept. They solved the first-order FDEs with the trapezoidal fuzzy initial condition. It gives good approximation results when using the minimal step size; otherwise, approximation results are not good. Ahmadian et al. [25] developed the RK method of fourth-order to solve first-order linear FIVPs. The advantages of the RK method include being a low order method which is more suitable and is used for temporal discretization of FDEs. The disadvantage of the RK method is that they are generally unsuitable for the solution of stiff equations as it increases the number of iteration steps [13].

Few researchers used the block method for the numerical solution of the FDEs. Mehrkanoon et al. [26] first developed the block method for the numerical solution of FDEs with FIVPs. They solved first-order FDEs by the proposed method. After that, Zawawi et al. [27] developed the diagonally implicit block backward differentiation

formula implemented in the predictor-corrector mode for the solution of first-order FIVPs with the advantage of solving two-steps simultaneously at one time. Ramli and Majid [28] proposed the implicit multistep block method and solved only first-order linear FDEs. Fook and Ibrahim [29] developed the two-points hybrid block method to solve first-order linear FDEs under Seikkala differentiable concept. Ramli and Majid [30] developed the fourth-order implicit diagonally multistep block method. They solved the linear and nonlinear FIVPs by this proposed method. Isa et al. [31] proposed a diagonally implicit multistep block method of order four and solved the linear and nonlinear first-order FIVPs. The major drawback in the group of studies highlighted is the implementation of the method as non-self-starting.

Generally, many researchers have developed various numerical methods to solve first-order FDEs with FIVPs. However, various gaps arise such as accuracy in terms of absolute error and self-starting issues in the solution of first-order FDEs. To address the drawbacks of the previously described numerical approaches (poor solution accuracy in terms of absolute error), this paper offers a one-step implicit numerical method with greater fuzzy derivatives for first-order FIVPs. The suggested method's convergence features, including consistency and zero-stability, are also studied. The created approach is then tested on numerical instances with beginning conditions specified as triangular and trapezoidal fuzzy numbers. Finally, the enhanced accuracy in terms of absolute error is reported in the numerical results section, as seen in the tables.

2. Ffuzzification of FIVP with OIS Method

A mathematical model can be expressed as an ODE system representing the dynamics of real-world problems. However, due to a model's unpredictable behaviour, uncertainty could arise in this situation, so an ODE system cannot be used as a reliable model. For this reason, FDEs are used to handle these situations [32].

Consider the first-order FIVP written as

$$D\tilde{\Omega}(t) = \tilde{\eta}(t, \tilde{\Omega}(t)),\ \tilde{\Omega}(t_0) = \tilde{\Omega}_0 \tag{1}$$

where $\tilde{\Omega}$ and $\tilde{\eta}$ are a fuzzy function of the crisp variable t, $D\tilde{\Omega}(t)$ is an H-derivative of $\tilde{\Omega}(t)$ and $\tilde{\Omega}(t_0)$ is a fuzzy initial value which is equal to the fuzzy number $\tilde{\Omega}_0$. Thus, the fuzzy function $\tilde{\Omega}$ is denoted as:

$$\left[\tilde{\Omega}(t)\right]_{\underline{\alpha}}^{\bar{\alpha}} = \left[\underline{\tilde{\Omega}}(t,\alpha), \bar{\tilde{\Omega}}(t,\alpha)\right],\ t \in T,\ \alpha \in [0,1] \tag{2}$$

and the α-cuts of $\tilde{\Omega}(t)$ is denoted as;

$$\begin{cases} \left[\tilde{\Omega}(t)\right]_{\underline{\alpha}}^{\bar{\alpha}} = \left[\underline{\tilde{\Omega}}(t,\alpha), \bar{\tilde{\Omega}}(t,\alpha)\right] \\ \left[\tilde{\Omega}(t_0)\right]_{\underline{\alpha}}^{\bar{\alpha}} = \left[\underline{\tilde{\Omega}}(t_0,\alpha), \bar{\tilde{\Omega}}(t_0,\alpha)\right] \end{cases} \tag{3}$$

Fuzzification is the method of converting a crisp quantity into a fuzzy quantity, and the inverse process of fuzzification is known as defuzzification. For defuzzification of first-order FIVPs, Equation (1) is written as

$$\left[\tilde{\eta}(t,\tilde{\Omega})\right]_{\underline{\alpha}}^{\bar{\alpha}} = \left[\underline{\tilde{\eta}}(t,\underline{\tilde{\Omega}};\alpha),\ \bar{\tilde{\eta}}(t,\bar{\tilde{\Omega}};\alpha)\right],\ t \in T,\ \alpha \in [0,1] \tag{4}$$

Here

$$\begin{cases} \underline{\tilde{\eta}}(t,\underline{\tilde{\Omega}};\alpha), = F\left[t, \underline{\tilde{\Omega}}(t), \bar{\tilde{\Omega}}(t)\right]_{\underline{\alpha}}^{\bar{\alpha}} \\ \bar{\tilde{\eta}}(t,\bar{\tilde{\Omega}};\alpha) = G\left[t, \underline{\tilde{\Omega}}(t), \bar{\tilde{\Omega}}(t)\right]_{\underline{\alpha}}^{\bar{\alpha}} \end{cases} \tag{5}$$

Since $D\tilde{\Omega}(t) = \tilde{\eta}(t, \tilde{\Omega}(t))$ is a fuzzy function, and F, G are nonlinear operator with the membership degree of $F\left[t, \underline{\tilde{\Omega}}(t), \bar{\tilde{\Omega}}(t)\right]_{\underline{\alpha}}^{\bar{\alpha}}$ and $G\left[t, \underline{\tilde{\Omega}}(t), \bar{\tilde{\Omega}}(t)\right]_{\underline{\alpha}}^{\bar{\alpha}}$ is defined as

$$\begin{cases} \underline{\tilde{\eta}}(t, \underline{\tilde{\Omega}}; \alpha) = min\left\{\tilde{\Omega}(t, \mu(t)) | \mu(t) \in D\tilde{\eta}(t, \underline{\tilde{\Omega}}(t, \alpha))\right\} \\ \bar{\tilde{\eta}}(t, \bar{\tilde{\Omega}}; \alpha) = \max\left\{\tilde{\Omega}(t, \mu(t)) | \mu(t) \in D\tilde{\eta}(t, \bar{\tilde{\Omega}}(t, \alpha))\right\} \end{cases} \tag{6}$$

and

$$\begin{cases} \underline{\tilde{\eta}}(t, \underline{\tilde{\Omega}}; \alpha) = F\left(t, \underline{\tilde{\Omega}}(t, \alpha), \bar{\tilde{\Omega}}(t, \alpha)\right) = F(t, \tilde{\Omega}(t, \alpha)) \\ \bar{\tilde{\eta}}(t, \bar{\tilde{\Omega}}; \alpha) = G\left(t, \underline{\tilde{\Omega}}(t, \alpha), \bar{\tilde{\Omega}}(t, \alpha)\right) = G(t, \tilde{\Omega}(t, \alpha)). \end{cases} \tag{7}$$

Given that the first-order FIVP of the form defined in Equation (1) be a mapping $\tilde{\eta} : \mathbb{R}_{\tilde{\eta}} \to \mathbb{R}_{\tilde{\eta}}$ and $\tilde{\Omega}_0 \in \mathbb{R}_{\tilde{\eta}}$ with an α-level set $\left[\tilde{\Omega}(t_0)\right]_{\underline{\alpha}}^{\bar{\alpha}} = \left[\underline{\tilde{\Omega}}(t_0, \alpha), \bar{\tilde{\Omega}}(t_0, \alpha)\right]$, $\alpha \in [0, 1]$, and with approximation solution denoted as $\left[\tilde{\Omega}(t)\right]_{\underline{\alpha}}^{\bar{\alpha}} = \left[\underline{\tilde{\Omega}}(t, \alpha), \bar{\tilde{\Omega}}(t, \alpha)\right]$, at which point, $h = \frac{t - t_0}{N}, t_n = t_0 + nh, 0 \leq n \leq N$. The expression to develop a second-third fuzzy derivatives OIS method for first-order FDEs using the Taylor Series block approach is obtained as

$$\tilde{\Omega}_{n+1}(t, \alpha) = \left(\tilde{\Omega}_n(t, \alpha) + \sum_{i=0}^{1} \left(\psi_{i1}\tilde{\eta}_{n+i}(t, \alpha) + \zeta_{i1}\tilde{\lambda}_{n+i}(t, \alpha) + \phi_{i1}\tilde{\delta}_{n+i}(t, \alpha)\right)\right)_{\underline{\alpha}}^{\bar{\alpha}} \tag{8}$$

Expanding Equation (8) leads to the expression in Equation (9)

$$\tilde{\Omega}_{n+1}(t, \alpha) = \begin{pmatrix} \tilde{\Omega}_n(t, \alpha) + \psi_{01}\tilde{\eta}_n(t, \alpha) + \psi_{11}\tilde{\eta}_{n+1}(t, \alpha) + \zeta_{01}\tilde{\lambda}_n(t, \alpha) + \zeta_{11}\tilde{\lambda}_{n+1}(t, \alpha) + \\ \phi_{01}\tilde{\delta}_n(t, \alpha) + \phi_{11}\tilde{\delta}_{n+1}(t, \alpha) \end{pmatrix}_{\underline{\alpha}}^{\bar{\alpha}} \tag{9}$$

Expending the individual term in Equation (9) by applying Taylor series expansion in fuzzy form as

$$\tilde{\Omega}_n = \left(\tilde{\Omega}(t_n, \alpha)\right)_{\underline{\alpha}}^{\bar{\alpha}},\ \tilde{\eta}_n = \left(\tilde{\Omega}'(t_n, \alpha)\right)_{\underline{\alpha}}^{\bar{\alpha}},\ \tilde{\lambda}_n = \left(\tilde{\Omega}''(t_n, \alpha)\right)_{\underline{\alpha}}^{\bar{\alpha}},\ \tilde{\delta}_n = \left(\tilde{\Omega}'''(t_n, \alpha)\right)_{\underline{\alpha}}^{\bar{\alpha}}$$

$$\tilde{\Omega}_{n+1} = \tilde{\Omega}(h; t_n, \alpha) = \left(\tilde{\Omega}(t_n, \alpha) + h\tilde{\Omega}'(t_n, \alpha) + \tilde{\Omega}''(t_n, \alpha)\frac{(h)^2}{2!} + \frac{(h)^3}{3!}\tilde{\Omega}'''(t_n, \alpha) + ... + \frac{(h)^n}{n!}\tilde{\Omega}^{(n)}(t_n, \alpha)\right)_{\underline{\alpha}}^{\bar{\alpha}}$$

$$\tilde{\eta}_{n+1} = \tilde{\eta}(h; t_n, \alpha) = \left(\tilde{\Omega}'(t_n, \alpha) + h\tilde{\Omega}''(t_n, \alpha) + \frac{(h)^2}{2!}\tilde{\Omega}'''(t_n, \alpha) + \frac{(h)^3}{3!}\tilde{\Omega}^{(iv)}(t_n, \alpha) + ... + \frac{(h)^n}{n!}\tilde{\Omega}^{(n)}(t_n, \alpha)\right)_{\underline{\alpha}}^{\bar{\alpha}}$$

$$\tilde{\lambda}_{n+1} = \tilde{\lambda}(h; t_n, \alpha) = \left(\tilde{\Omega}''(t_n, \alpha) + h\tilde{\Omega}'''(t_n, \alpha) + \frac{(h)^2}{2!}\tilde{\Omega}^{(iv)}(t_n, \alpha) + \frac{(h)^3}{3!}\tilde{\Omega}^{(v)}(t_n, \alpha) + ... + \frac{(h)^n}{n!}\tilde{\Omega}^{(n)}(t_n, \alpha)\right)_{\underline{\alpha}}^{\bar{\alpha}}$$

$$\tilde{\delta}_{n+1} = \tilde{\delta}(h; t_n, \alpha) = \left(\tilde{\Omega}'''(t_n, \alpha) + h\tilde{\Omega}^{(iv)}(t_n, \alpha) + \frac{(h)^2}{2!}\tilde{\Omega}^{(v)}(t_n, \alpha) + \frac{(h)^3}{3!}\tilde{\Omega}^{(v)}(t_n, \alpha) + ... + \frac{(h)^n}{n!}\tilde{\Omega}^{(n)}(t_n, \alpha)\right)_{\underline{\alpha}}^{\bar{\alpha}}$$

$$\begin{pmatrix} (\tilde{\Omega}(t_n, \alpha) + h\tilde{\Omega}'(t_n, \alpha) + \tilde{\Omega}''(t_n, \alpha)\frac{(h)^2}{2!} + \frac{(h)^3}{3!}\tilde{\Omega}'''(t_n, \alpha) + ...) - \tilde{\Omega}(t_n, \alpha) - \\ \psi_{01}\tilde{\Omega}'(t_n, \alpha) - \psi_{11}(\tilde{\Omega}'(t_n, \alpha) + h\tilde{\Omega}''(t_n, \alpha) + \frac{(h)^2}{2!}\tilde{\Omega}'''(t_n, \alpha) + \frac{(h)^3}{3!}\tilde{\Omega}^{(iv)}(t_n, \alpha) + ...) - \\ \zeta_{01}\tilde{\Omega}''(t_n, \alpha) - \zeta_{11}(\tilde{\Omega}''(t_n, \alpha) + h\tilde{\Omega}'''(t_n, \alpha) + \frac{(h)^2}{2!}\tilde{\Omega}^{(iv)}(t_n, \alpha) + \frac{(h)^3}{3!}\tilde{\Omega}^{(v)}(t_n, \alpha) + ...) - \\ \phi_{01}\tilde{\Omega}'''(t_n, \alpha)_n - \phi_{11}(\tilde{\Omega}'''(t_n, \alpha) + h\tilde{\Omega}^{(iv)}(t_n, \alpha) + \frac{(h)^2}{2!}\tilde{\Omega}^{(v)}(t_n, \alpha) + \frac{(h)^3}{3!}\tilde{\Omega}^{(v)}(t_n, \alpha) + ...) \end{pmatrix}_{\underline{\alpha}}^{\bar{\alpha}} = 0$$

and rewriting in matrix form by equating coefficients of $\tilde{\Omega}^{(n)}(t_n;\alpha)$ and the values of the coefficients are obtained using the matrix inverse method, and the result is given below,

$$\left[\begin{pmatrix}\psi_{01}\\ \psi_{11}\\ \xi_{01}\\ \xi_{11}\\ \phi_{01}\\ \phi_{11}\end{pmatrix} = \begin{pmatrix}1 & 1 & 0 & 0 & 0 & 0\\ 0 & h & 1 & 1 & 0 & 0\\ 0 & \frac{h^2}{2!} & 0 & h & 1 & 1\\ 0 & \frac{h^3}{3!} & 0 & \frac{h^2}{2!} & 0 & h\\ 0 & \frac{h^4}{4!} & 0 & \frac{h^3}{3!} & 0 & \frac{h^2}{2!}\\ 0 & \frac{h^5}{5!} & 0 & \frac{h^4}{4!} & 0 & \frac{h^3}{3!}\end{pmatrix}^{-1} \times \begin{pmatrix}h\\ \frac{h^2}{2!}\\ \frac{h^3}{3!}\\ \frac{h^4}{4!}\\ \frac{h^5}{5!}\\ \frac{h^6}{6!}\end{pmatrix} = \begin{pmatrix}\frac{h}{2}\\ \frac{h}{2}\\ \frac{h^2}{10}\\ \frac{h^2}{10}\\ \frac{h^3}{120}\\ \frac{h^3}{120}\end{pmatrix}\right]_{\underline{\alpha}}^{\overline{\alpha}}$$

Substituting these values in Equation (9) gives the one-step second-third derivatives method as

$$\tilde{\Omega}_{n+1}(t,\alpha) = \begin{pmatrix}\tilde{\Omega}_n(t,\alpha) + \frac{h}{2}\left(\tilde{\eta}_n(t,\alpha) + \tilde{\eta}_{n+1}(t,\alpha)\right) + \frac{h^2}{10}\left(\tilde{\lambda}_n(t,\alpha) - \tilde{\lambda}_{n+1}(t,\alpha)\right) +\\ \frac{h^3}{120}\left(\tilde{\delta}_n(t,\alpha) - \tilde{\delta}_{n+1}(t,\alpha)\right)\end{pmatrix}_{\underline{\alpha}}^{\overline{\alpha}} \tag{10}$$

Following Equation (11), the correctors of the block method in Equation (10) take the form,

$$\left(A^0\widetilde{Y}_{n+1} = A^1\widetilde{Y}_{n-1} + h(B^0\widetilde{F}_{n-1} + B^1\widetilde{F}_{n+1}) + h^2(C^0\widetilde{G}_{n-1} + C^1\widetilde{G}_{n+1}) + h^3(E^0\widetilde{M}_{n-1} + E^1\widetilde{M}_{n+1})\right)_{\underline{\alpha}}^{\overline{\alpha}} \tag{11}$$

$$\left[\begin{array}{l}A^0 = (1), A^1 = (1), B^0 = \left(\frac{1}{2}\right), B^1 = \left(\frac{1}{2}\right), C^0 = \left(\frac{1}{10}\right), C^1 = \left(\frac{1}{10}\right), D^0 = \left(\frac{1}{120}\right), D^1 = \left(\frac{1}{120}\right),\\ \tilde{Y}_{n+1} = \left(\tilde{\Omega}_{n+1}\right), \tilde{Y}_{n-1} = \left(\tilde{\Omega}_n\right), \tilde{F}_{n+1} = (\tilde{\eta}_{n+1}), \tilde{F}_{n-1} = (\tilde{\eta}_n), \tilde{G}_{n+1} = \left(\tilde{\lambda}_{n+1}\right), \tilde{G}_{n-k} = \left(\tilde{\lambda}_n\right),\\ \tilde{M}_{n+1} = \left(\tilde{\delta}_{n+1}\right), \tilde{M}_{n-1} = \left(\tilde{\delta}_n\right).\end{array}\right]_{\underline{\alpha}}^{\overline{\alpha}}$$

3. Theoretical Properties of the OIS

The following properties of the OIS are discussed in this section: order, zero-stability, consistency, and region of absolute stability.

3.1. Order of the OIS

Following the steps in [34] to expand individual terms of the obtained OIS in Equation (10) using Taylor series expression gives

$$\begin{pmatrix}(\tilde{\Omega}(t_n,\alpha) + h\tilde{\Omega}'(t_n,\alpha) + \frac{h^2}{2!}\tilde{\Omega}''(t_n,\alpha) + \frac{h^3}{3!}\tilde{\Omega}'''(t_n,\alpha) + \frac{h^4}{4!}\tilde{\Omega}^{(iv)}(t_n,\alpha) + \frac{h^5}{5!}\tilde{\Omega}^{(v)}(t_n,\alpha) +\\ \frac{h^6}{6!}\tilde{\Omega}^{(vi)}(t_n,\alpha) + \frac{h^7}{7!}\tilde{\Omega}^{(vii)}(t_n,\alpha) + ...) - \tilde{\Omega}(t_n,\alpha) - \frac{h}{2}(\tilde{\Omega}'(t_n,\alpha) + \tilde{\Omega}'(t_n,\alpha) + h\tilde{\Omega}''(t_n,\alpha) +\\ \frac{h^2}{2!}\tilde{\Omega}'''(t_n,\alpha) + \frac{h^3}{3!}\tilde{\Omega}^{(iv)}(t_n,\alpha) + \frac{h^4}{4!}\tilde{\Omega}^{(v)}(t_n,\alpha) + \frac{h^5}{5!}\tilde{\Omega}^{(vi)}(t_n,\alpha) + \frac{h^6}{6!}\tilde{\Omega}^{(vii)}(t_n,\alpha) + ...)) -\\ \frac{h^2}{10}(\tilde{\Omega}''(t_n,\alpha) - (\tilde{\Omega}''(t_n,\alpha) + h\tilde{\Omega}'''(t_n,\alpha) + \frac{h^2}{2!}\tilde{\Omega}^{(iv)}(t_n,\alpha) + \frac{h^3}{3!}\tilde{\Omega}^{(v)}(t_n,\alpha) + \frac{h^4}{4!}\tilde{\Omega}^{(vi)}(t_n,\alpha)\\ + \frac{h^5}{5!}\tilde{\Omega}^{(vii)}(t_n,\alpha) + ...)) - \frac{h^3}{120}(\tilde{\Omega}'''(t_n,\alpha) + \tilde{\Omega}'''(t_n,\alpha) + h\tilde{\Omega}^{(iv)}(t_n,\alpha) + \frac{h^2}{2!}\tilde{\Omega}^{(v)}(t_n,\alpha) +\\ \frac{h^3}{3!}\tilde{\Omega}^{(vi)}(t_n,\alpha) + \frac{h^4}{4!}\tilde{\Omega}^{(vii)}(t_n,\alpha) + ...) = 0\end{pmatrix}_{\underline{\alpha}}^{\overline{\alpha}} \tag{12}$$

Equating the coefficients of in Equation (12), the order of the method is computed as

$$\begin{pmatrix} 1 \\ 1 \\ \frac{1}{2!} \\ \frac{1}{3!} \\ \frac{1}{4!} \\ \frac{1}{5!} \\ \frac{1}{6!} \\ \frac{1}{7!} \end{pmatrix} - \begin{pmatrix} 1 \\ 0 \\ 0 \\ 0 \\ 0 \\ 0 \\ 0 \\ 0 \end{pmatrix} - \frac{1}{2}\left[\begin{pmatrix} 0 \\ 1 \\ 0 \\ 0 \\ 0 \\ 0 \\ 0 \\ 0 \end{pmatrix} + \begin{pmatrix} 0 \\ 1 \\ 1 \\ \frac{1}{2!} \\ \frac{1}{3!} \\ \frac{1}{4!} \\ \frac{1}{5!} \\ \frac{1}{6!} \end{pmatrix}\right] - \frac{1}{10}\left[\begin{pmatrix} 0 \\ 0 \\ 1 \\ 0 \\ 0 \\ 0 \\ 0 \\ 0 \end{pmatrix} - \begin{pmatrix} 0 \\ 0 \\ 1 \\ 1 \\ \frac{1}{2!} \\ \frac{1}{3!} \\ \frac{1}{4!} \\ \frac{1}{5!} \end{pmatrix}\right] - \frac{1}{120}\left[\begin{pmatrix} 0 \\ 0 \\ 0 \\ 1 \\ 0 \\ 0 \\ 0 \\ 0 \end{pmatrix} + \begin{pmatrix} 0 \\ 0 \\ 0 \\ 1 \\ 1 \\ \frac{1}{2!} \\ \frac{1}{3!} \\ \frac{1}{4!} \end{pmatrix}\right] = \begin{pmatrix} 0 \\ 0 \\ 0 \\ 0 \\ 0 \\ 0 \\ 0 \\ -9.9206e-06 \end{pmatrix}$$

Thus, the order of the OIS method is $q = 6$ with error constant value $C_7 = (-9.9206e - 06)$ and principal LTE $C_7 h^{(7)} \tilde{\Omega}^{(7)}(t_n, \alpha)$.

3.2. Consistency

Following steps [35] to test the OIS for zero-stability, the corrector of the method is normalized according to Equation (11) to give the first characteristic polynomial $P(\phi)$ as

$$P(\phi) = det(\phi_\eta A^0 - A^1) = |(\phi)\,(1) - (1)| = \phi - 1 = 0,\ with\ \phi = 1.$$

which is a simple root. So, the OIS is zero-stable. Likewise, since the OIS is consistent and zero-stable, according to [], the developed method is convergent.

3.3. Region of Absolute Stability

Following [34] the stability polynomial for the OIS takes the form

$$R(w) = \left|[-w] + [1] + q\left[\tfrac{w}{2} + \tfrac{1}{2}\right] + q^2\left[\tfrac{1}{10} - \tfrac{w}{10}\right] + q^3\left[\tfrac{1}{120} - \tfrac{w}{120}\right]\right|_{\underline{\alpha}}^{\bar{\alpha}}$$

$$R(w) = (1 + \tfrac{q}{2} - \tfrac{q^2}{10} - \tfrac{q^3}{120})w + 1 + \tfrac{q}{2} + \tfrac{q^2}{10} + \tfrac{q^3}{120} \tag{13}$$

The region of absolute stability of Equation (13) is plotted using the boundary locus approach, as shown in Figure 1 below Figure 1 demonstrates the interval of the stability region and that all the polynomial roots for the absolute

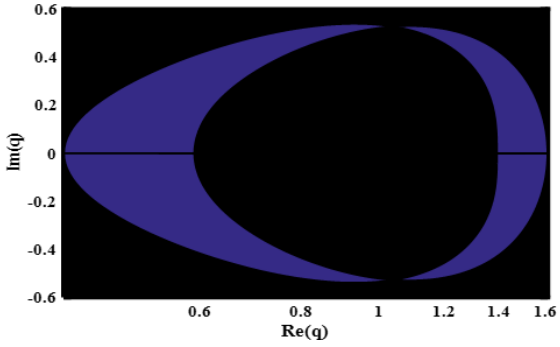

Figure 1. Absolute Stability Region of OIS

stability region are located on the unit circle, which indicates that the large step-size h value selected can be used to the OIS.

4. Implementation of the OIS for Real life Models

The derivatives of the supplied first-order FDEs are first acquired from the given numerical problems to implement the established OIS for solving first-order FDEs. Subsequently, the parameters are transformed into the fuzzy numbers' parametric form (α-level). After that, the conditions $t_n,\ n = 0, 1, ..., N$ produces two solutions $\tilde{\Omega}(t_n, \alpha) = \left(\underline{\tilde{\Omega}}(t_n, \alpha), \bar{\tilde{\Omega}}(t_n, \alpha)\right)$, known as lower and upper solutions respectively. To test the accuracy of the OIS developed above, the following first-order real-life models are considered

4.1. Model 1. Liquid Tank System 36

A tank system is shown in Figure 2. Presume that the tank's inflow disturbances are $I = t + 1$ what cause the

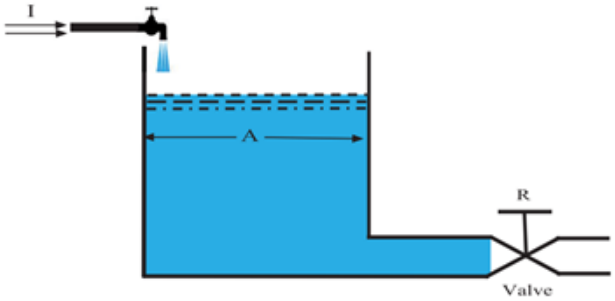

Figure 2. Liquid Tank System

vibration at the liquid level x, where $R = 1$ the flow obstruction lies and where the valve may be used to reduce it. is the tank's cross-section is $A = 1$, and the liquid level is represented by

$$D\tilde{\Omega}(t, \alpha) = -\frac{1}{AR}\tilde{\Omega}(t, \alpha) + \frac{1}{A} \tag{14}$$

With second third derivatives $D'\tilde{\Omega}(t, \alpha) = -\frac{1}{AR}D\tilde{\Omega}(t, \alpha)$, and $D''\tilde{\Omega}(t, \alpha) = -\frac{1}{AR}D'\tilde{\Omega}(t, \alpha)$ The initial condition is $\tilde{\Omega}(0, \alpha) = (0.96 + 0.04\alpha, 1.01 - 0.01\alpha),\ \alpha \in [0, 1]$, then the exact solution of Equation (14) is $\tilde{\partial}(t, \alpha) = (0.96 + 0.04\alpha,\ 1.01 - 0.01\alpha)e^{-t} + t$, where $t \in [0, 1]$,and $h = 0.1$. The OIS is used to approximate the solution of Equation (14) and compared with [16], where SNN, and DNN were presented. The solution's accuracy in terms of absolute error with lower and upper bounds is presented in Table 1 at $t = 1$. The results in Table 1 show the developed OIS in this study having improved accuracy in terms of absolute error. Figure 3 shows the 3-dimensional solution via developed OIS for model 1. Figures 4, and 5 display the computed approximate solutions using the OIS to show the uncertain behaviour of the liquid tank system with different values of $\alpha \in [0, 1]$. According to Figures

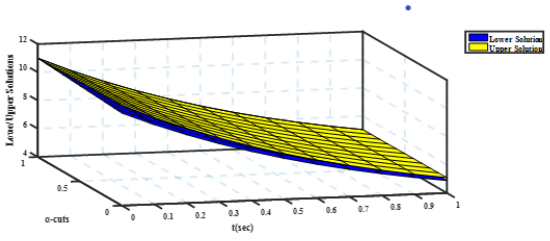

Figure 3. The 3-Dimensional solution via developed OIS for model 1 for all $t, \alpha \in [0, 1]$.

Table 1. Comparison of the OIS with [16] for Solving Model 1.

α	OIS Lower Approximate solution	SNN Absolute Error	DNN Absolute Error	OIS Absolute Error
0	1.353164263524584600	3.8700e-02	7.0100e-02	4.4509e-17
0.2	1.356107299053956200	4.5100e-02	7.7100e-02	4.4509e-17
0.4	1.359050334583327800	N/A	N/A	2.2504e-17
0.6	1.361993370112699200	N/A	N/A	4.4509e-17
0.8	1.364936405642070700	5.5400e-02	6.4900e-02	4.4509e-17
1	1.367879441171442300	5.5400e-02	9.0100e-02	4.4509e-17
α	OIS Lower Approximate solution	SNN Absolute Error	DNN Absolute Error	OIS Absolute Error
0	1.371558235583156800	8.8400e-02	1.0120e-01	4.4509e-17
0.2	1.370822476700813900	8.8400e-02	1.2010e-01	4.4509e-17
0.4	1.370086717818471000	N/A	N/A	4.4509e-17
0.6	1.369350958936128100	N/A	N/A	4.4509e-17
0.8	1.368615200053785200	6.3500e-02	8.1200e-02	4.4509e-17
1	1.367879441171442300	5.5400e-02	9.0100e-02	4.4509e-16

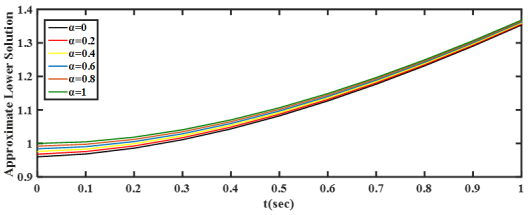

Figure 4. Uncertain Behaviour of the model 1 using OIS with Lower Bound

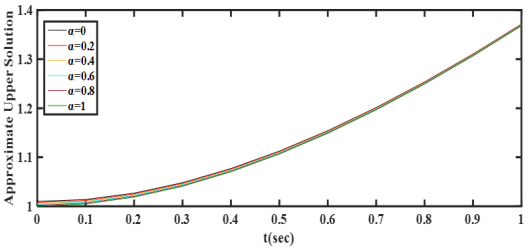

Figure 5. Uncertain Behaviour of the model 1 using OIS with Upper Bound

3 and 5, the solution (membership values with α-cuts) of the liquid tank system model in Equation (14) increases with the lower bound and decreases with the upper bound. In addition, the use of the triangular fuzzy number for the initial condition of the liquid tank system model was a range of $[0.96,\ 1.01]$ for time t. This gives more information for the approximate solution $\tilde{\Omega}(t)$ of the model such that over initial condition $\tilde{\Omega}(0) = (0.96,\ 1,\ 1.01)$, $\tilde{\Omega}(t) = (1.353,\ 1.368,\ 1.372)$ correspondingly.

4.2. Model 2. Thermal System [36]

Figure 6 shown a tank with a heating system. Assume $R = 0.5$ is the flow obstruction, $C = 2$ the thermal capacitance, and the temperature a time is $\tilde{\Omega}(t)$. The model is

$$D\tilde{\Omega}(t,\alpha) = -\frac{1}{RC}\tilde{\Omega}(t,\alpha) \tag{15}$$

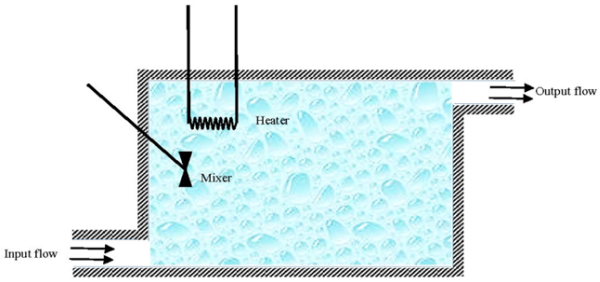

Figure 6. Thermal System

With second-third derivatives $D'\tilde{\Omega}(t,\alpha) = -\frac{1}{RC}D\tilde{\Omega}(t,\alpha)$ and $D''\tilde{\Omega}(t,\alpha) = -\frac{1}{RC}D'\tilde{\Omega}(t,\alpha)$ where $t \in [0,4]$. If the initial condition is $\tilde{\Omega}(t,\alpha) = (\alpha-1,\ 1-\alpha)$, $\alpha \in [0,1]$, then the exact solution of Equation (15) is $\tilde{\partial}(t,\alpha) = (\alpha-1,\ 1-\alpha)e^{-t}$. The OIS is used to approximate the solution of Equation (15) and compared with the SNN and DNN methods in [16]. Table 2 displays the solution's accuracy regarding absolute error, including both lower and upper bounds, for $t = 1$ and $h = 0.1$. The results in Table 2 show the developed OIS in this study having

Table 2. Comparison of the OIS with [16] for Solving Model 2

α	OIS Lower Approximate solution	SNN Absolute Error	DNN Absolute Error	OIS Absolute Error
0	-0.367879441171442330	4.0700e-02	1.8400e-02	2.2304e-17
0.2	-0.294303552937153880	3.5100e-02	2.5100e-02	1.6453e-17
0.4	-0.220727664702865390	3.3400e-02	1.1100e-02	1.3578e-17
0.6	-0.147151776468576940	2.8200e-02	1.0400e-02	8.3667e-18
0.8	-0.073575888234288470	2.5300e-02	1.0200e-02	6.9789e-18
1	0.000000000000000000	3.2300e-02	1.1200e-02	0
α	OIS Lower Approximate solution	SNN Absolute Error	DNN Absolute Error	OIS Absolute Error
0	0.367879441171442330	6.0400e-02 3.1700e-02	2.2304e-17	
0.2	0.294303552937153880	5.7800e-02	1.0500e-02	1.6353e-17
0.4	0.220727664702865390	5.2300e-02	2.8400e-02	1.3478e-17
0.6	0.147151776468576940	4.1700e-02	3.0100e-02	8.3567e-17
0.8	0.073575888234288470	5.0100e-02	3.1300e-02	6.9689e-18
1	0.000000000000000000	3.2300e-02	1.1200e-02	0

improved accuracy in terms of absolute error. Figure 7 shows the 3-dimensional solution via developed OIS for model 2. Figures 8, and 9 display the computed approximate solutions using the OIS to show the uncertain behaviour of the tank thermal system with time interval $[0,4]$ and different values of $\alpha \in [0,1]$. According to

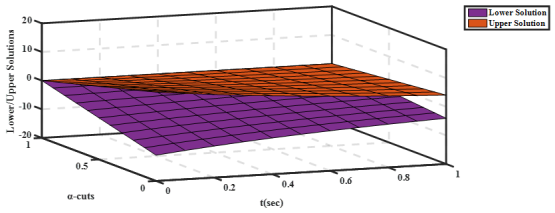

Figure 7. The 3-Dimensional solution via developed OIS for model 2 for all $t, \alpha \in [0,1]$.

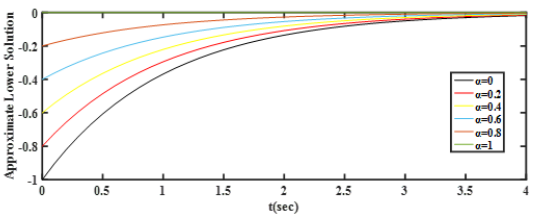

Figure 8. Uncertain Behaviour of the model 2 using OIS with Lower Bound

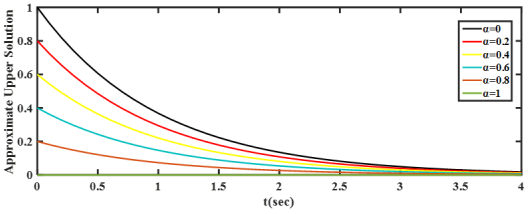

Figure 9. Uncertain Behaviour of the model 2 using OIS with Upper Bound

Figures 8 and 9, the solution (membership values with α-cuts) of the thermal system model in Equation (15) increases with the lower bound and decreases with the upper bound. In addition, the use of the triangular fuzzy number for the initial condition of the thermal system model was a range of $[-1,\ 1]$. for time t. This gives more information for the approximate solution $\tilde{\Omega}(t)$ of the model such that over initial condition $\tilde{\Omega}(0) = (-1, 0,\ 1)$, $\tilde{\Omega}(t) = (-0.368,\ 0,\ 0.368)$ correspondingly.

4.3. Model 3. Nuclear decay [33]

Consider the nuclear decay equation

$$\frac{d\Omega(t)}{dt} = -\lambda\Omega(t), \Omega(t_0) = \Omega_0, t \in I = [t_0, \alpha] \tag{16}$$

where the number of radionuclides present in a radioactive material is $\Omega(t)$, the decay constant is λ and the initial number Ω_0 of radionuclides. If we don't know for sure how many radionuclides are initially present in the material, uncertainty is included to the model. Keep in mind that nuclear disintegration is seen as a stochastic process, and that the lack of knowledge about the radioactive substance being studied adds uncertainty to the process. On the other hand, there can occasionally be uncertainty regarding the quantity of radionuclides contained in the radioactive substance. To consider the uncertainty and hesitation; consider Ω_0 to be a triangular intuitionistic fuzzy number. Let $\lambda = 1$, $I = [0,\ 4]$, and $\Omega_0 = (0.75,\ 1,\ 1.125)$.Then Equation (16) in fuzzy form is defined as

$$\frac{d\tilde{\Omega}(t)}{dt} = -\tilde{\Omega}(t),\ \tilde{\Omega}(t_0) = (0.75 + 0.25\alpha,\ 1, 125 - 0.125\alpha). \tag{17}$$

The exact solution of Equation (17) is $\tilde{\partial}(t, \alpha) = (0.75 + 0.25\alpha,\ 1.125 - 0.125\alpha)e^t,\ \alpha \in [0, 1]$. The OIS is used to approximate the solution of Equation (17) and the solution is compared with [34], where the general linear method (GLM) and RK method were presented. The solution's accuracy in terms of absolute error with lower and upper bounds is presented in Table 3 at $t = 1$, and $h = 0.1$. The results in Table 3 show the developed OIS in this study having improved accuracy in terms of absolute error. Figure 10 shows the 3-dimensional solution via developed OIS for model 2. Figures 11, and 12 display the computed approximate solutions using the OIS to show the uncertain behaviour of the model 3 with time interval $[0, 4]$ and different values of $\alpha \in [0, 1]$. According to

Table 3. Comparison of the OIS with, [34] for Solving Model 3.

α	OIS Lower Approximate solution	GLM Absolute Error	RK Absolute Error	OIS Absolute Error
0	2.038711371344283900	5.2917e-10	1.8281e-06	1.3223e-16
0.2	2.174625462767236300	4.2322e-10	1.4625e-06	1.7264e-16
0.4	2.310539554190188300	3.1750e-10	1.0969e-06	1.7264e-16
0.6	2.446453645613140700	2.1166e-10	7.3127e-07	1.7264e-16
0.8	2.582367737036093100	1.0583e-10	3.6563e-07	1.7264e-16
1	2.718281828459045100	0	0	0
α	OIS Lower Approximate solution	GLM Absolute Error	RK Absolute Error	OIS Absolute Error
0	3.058067057016426100	5.2917e-10	1.8281e-06	2.2304e-16
0.2	2.990110011304949900	4.2322e-10	1.4625e-06	2.2504e-16
0.4	2.922152965593473700	3.1750e-10	1.0969e-06	2.2304e-16
0.6	2.854195919881997500	2.1166e-10	7.3127e-07	2.2504e-16
0.8	2.786238874170521300	1.0583e-10	3.6563e-07	1.7564e-16
1	2.718281828459045100	0	0	0

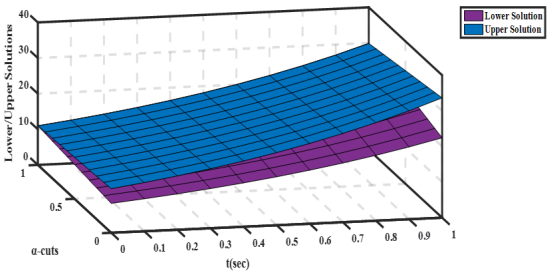

Figure 10. The 3-Dimensional solution via developed OIS for model 3 for all $t, \alpha \in [0, 1]$.

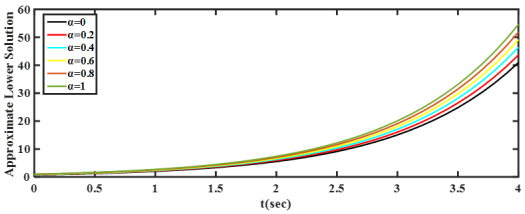

Figure 11. Uncertain Behaviour of the model 3 using OIS with Lower Bound

Figures 11 and 12, the solution (membership values with α-cuts) of the thermal system model in Equation (15) increases with the lower bound and decreases with the upper bound. In addition, the use of the triangular fuzzy number for the initial condition of the thermal system model was a range of $[0.75,\ 1.125]$ for time t. This gives more information for the approximate solution $\tilde{\Omega}(t)$ of the model such that over initial condition $\tilde{\Omega}(0) = (0.75,\ 1,\ 1.125)$, $\tilde{\Omega}(t) = (2.0387,\ 2.718,\ 3.058)$ correspondingly.

4.4. Model 4. SIR Model [33]

The potential number of individuals infected with an infectious disease over time in a closed community is calculated using the SIR model, an epidemiological model. The fact that these linked equations relate the numbers of susceptible individuals $S(t)$, infected individuals$I(t)$, and recovered individuals $R(t)$, gives rise to the moniker

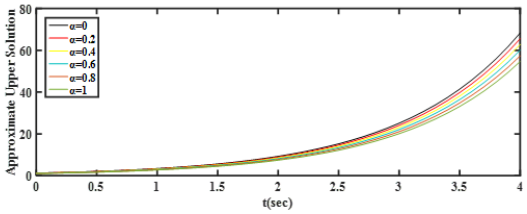

Figure 12. Uncertain Behaviour of the model 3 using OIS with Upper Bound

of this class of models. For several infectious illnesses, such as the measles, mumps, and rubella, this is an effective and basic approach. It is given by the following three coupled equations:

$$\begin{cases} \dfrac{dS}{dt} = \mu(1-S) - \beta IS \\ \dfrac{dI}{dt} = \mu I - \gamma I + \beta IS \\ \dfrac{dR}{dt} = -\mu R + \gamma I \end{cases} \tag{18}$$

where, μ, β, and γ, are positive parameters. Define Ω to be

$$\Omega = I + S + R \tag{19}$$

the evolution equation following for Ω

$$\Omega' = \mu(1-\Omega) \tag{20}$$

Taking $\mu = 0.5$ for an initial condition (for a particular closed population), To consider, the uncertainty and hesitation; Ω_0 being a triangular intuitionistic fuzzy number. Let $\mu = 0.5$ and $t \in [0,\ 1]$, $\tilde{\Omega}_0 = (0,\ 0.5,\ 1)$. Then Equation (20) in fuzzy form defines as

$$\tilde{\Omega}' = \mu(1-\tilde{\Omega}) \tag{21}$$

The exact solution of Equation (21) is $\tilde{\partial}(t,\alpha) = (1-0.5\alpha,\ 1-(1-0.5\alpha))e^{-0.5t}$, $\alpha \in [0,1]$. The OIS used to approximate the solution Equation (21). The solution of this SIR model as a FIVP is compared with [35] at $\alpha = 1$, where the two-step implicit Obrechkoff-type block method (2SBM) solved this model in crisp form. The solution's accuracy in terms of absolute error with lower and upper bounds is presented in Table 4 at $t = 1$, and $h = 0.1$. The

Table 4. Comparison of the OIS with [35] for Solving Model 4.

α	OIS Lower solution	2SBM Error	OIS Error	OIS Upper solution	2SBM Error	OIS Error
0	1.0000000000000	N/A	0	0.393469340287	N/A	0
0.2	0.9393469340287	N/A	0	0.454122406256	N/A	0
0.4	0.8786938680574	N/A	0	0.514775472229	N/A	0
0.6	0.8180408020862	N/A	0	0.575428538201	N/A	0
0.8	0.7573877361149	N/A	0	0.636081604172	N/A	0
1	0.6967346701436	2.520e-13	0	0.696734670143	2.5e-13	0

results in Table 4 show the developed OIS in this study having improved accuracy in terms of absolute error. Figure 13 shows the 3-dimensional solution via developed OIS for model 4. Figures 14, and 15 display the computed approximate solutions using the OIS to show the uncertain behaviour of the model 4 with time interval $[0, 10]$ and

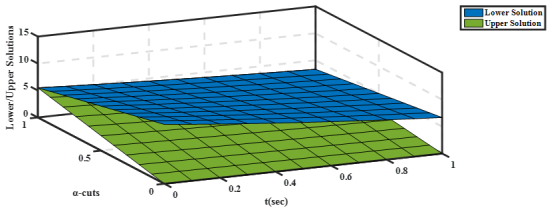

Figure 13. The 3-Dimensional solution via developed OIS for model 4 for all $t, \alpha \in [0, 1]$.

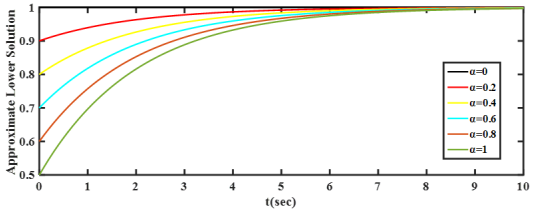

Figure 14. Uncertain Behaviour of the model 4 using OIS with Lower Bound

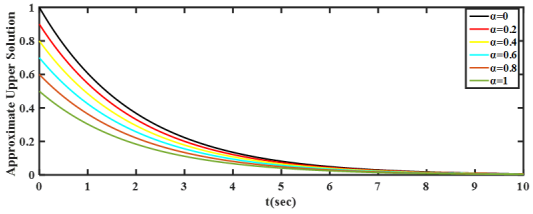

Figure 15. Uncertain Behaviour of the model 4 using OIS with Upper Bound

different values of $\alpha \in [0, 1]$. According to Figures 14 and 15, the solution (membership values with α-cuts of the thermal system model in Equation (21) decreases with the lower bound and increases with the upper bound. In addition, the use of the triangular fuzzy number for the initial condition of the thermal system model was a range of decreases for time$t$. This gives more information for the approximate solution $\tilde{\Omega}(t)$ of the model such that over initial condition $\tilde{\Omega}(0) = (0,\ 0.5,\ 1)$, $\tilde{\Omega}(t) = (1,\ 0.697,\ 0.395)$ correspondingly.

4.5. Model 5. Charging and Discharging Capacitor

Consider the following crisp capacitor model in [33]

$$\frac{d(U_c(t))}{dt} = -\frac{1}{RC}U_c(t) + \frac{1}{RC}U_G(t) \tag{22}$$

with exact solution

$$U_c(t) = K.e^{-\int \frac{dt}{RC}} + \left[\int (\frac{U_G(t)}{RC}.e^{-\int \frac{dt}{RC}})dt\right].e^{-\int \frac{dt}{RC}} \tag{23}$$

For the initial condition used in the case of charging of the capacitor is $U_C(0) = 0$.

$$U_C(t) = U_B.[1 - e^{\frac{t}{RC}}] \tag{24}$$

while the initial condition used in the case of discharging of the capacitor $U_C(0) = U_0$

$$U_C(t) = U_{c,0}.e^{\frac{t}{RC}} \tag{25}$$

[36, 37, 38] state that the fuzzy theory's formulation may be used to describe the crisp equation in a fuzzy manner. Hence, triangular fuzzy numbers are used to characterize the erratic behavior of a capacitor when it uses the voltage, capacitance, or resistance of the circuit current. The following capacitor model in fuzzy form as stated blow

$$\frac{d(\widetilde{U}_c(t))}{dt} = -\frac{1}{RC}\widetilde{U}_c(t) + \frac{1}{RC}\widetilde{U}_G(t) \tag{26}$$

with exact solution

$$\widetilde{U}_c(t) = K.e^{-\int \frac{dt}{RC}} + \left[\int (\frac{\widetilde{U}_G(t)}{RC}.e^{-\int \frac{dt}{RC}})dt\right].e^{-\int \frac{dt}{RC}}. \tag{27}$$

charging of the capacitor for the fuzzy initial condition

$$\widetilde{U}_C(t) = \widetilde{U}_B.[1 - e^{\frac{t}{RC}}] \tag{28}$$

while the fuzzy initial condition discharging of the capacitor

$$\widetilde{U}_C(t) = \widetilde{U}_{c,0}.e^{\frac{t}{RC}}. \tag{29}$$

Charging of a Capacitor. The solutions are presented at $t = 4s$,with the triangle fuzzy number, Table 8.5 displays the accuracy of the bottom and upper solutions for charging a capacitor in a DC state. The resulting graphs, with battery voltage set to $12V$, $C = 0.25F$, $U_c(0) = 0$, and resistance with triangular fuzzy number is $R = (2 + \alpha,\ 4 - \alpha)$, $\alpha = [0,\ 1]$ are displayed in Figures 17 and 18.

Discharging of a Capacitor. The solutions are presented at $t = 4s$, with the triangle fuzzy number, Table 8.5 displays the accuracy of the bottom and upper solutions for discharging a capacitor in a DC state. The resulting graphs, with battery voltage set to $12V$, $C = 0.25F$, $U_c(0) = 12V$, and resistance with triangular fuzzy number is $R = (2 + \alpha,\ 4 - \alpha)$, $\alpha = [0,\ 1]$ are displayed in Figures 21 and 20. The OIS with FIVP was successfully used to

Table 5. Comparison of the OIS with Exact Solution for Solving Charging of Capacitor Model 5.

α	OIS Lower solution	OIS absolute Error	OIS Upper solution	OIS absolute Error
0	11.995974448465169	0	11.780212333335189	0
0.2	11.991669406884018	0	11.821937321808754	0
0.4	11.984728394383922	0	11.859076458515744	0
0.6	11.974496498029186	0	11.905917027388661	0
0.8	11.960417930928731	0	11.931188450176629	0
1	11.942064600074023	0	11.942064600074023	0

Table 6. Comparison of the OIS with Exact Solution for Solving Discharging of Capacitor Model 5.

α	OIS Lower solution	OIS absolute Error	OIS Upper solution	OIS absolute Error
0	0.0040255515348301	4.33680e-18	0.2197876666648101	8.32667e-17
0.2	0.0083305931159827	7.80626e-18	0.1780626781912458	8.32667e-17
0.4	0.0152716056160777	8.67317e-18	0.1409235414842563	1.94289e-16
0.6	0.0255035019708145	1.73723e-18	0.1085031902559575	2.22044e-16
0.8	0.0395820690712690	1.00834e-17	0.0808553639890256	8.32663e-17
1	0.0579353999259772	1.04834e-17	0.0579353999259772	1.52655e-16

solve the crisp capacitor model, and the outcomes were compared to the precise solution. Tables 5 and 6 display the estimated outcomes of charging and discharging the capacitor, respectively. Figures 16-21 show the computed

approximate solutions using the OIS developed in this study to illustrate the uncertain behavior of the charging and discharging capacitor model with various values of $\alpha \in [0, 1]$. The tables show that the accuracy of the solution in term of absolute error is very high. Capacitor is fully charged when the uncertain parameter $\alpha = 0$ and it is also

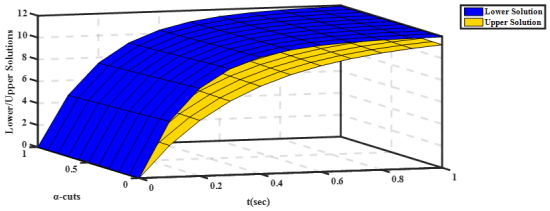

Figure 16. The 3-Dimensional solution via developed OIS for model 5 with Charging for all $t, \alpha \in [0, 1]$.

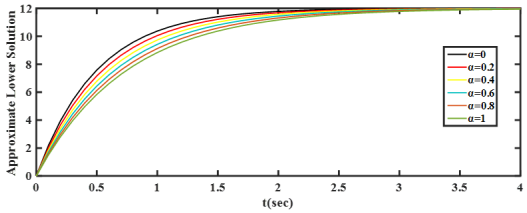

Figure 17. Uncertain Behaviour of the model 5 using OIS with Charging Lower Bound

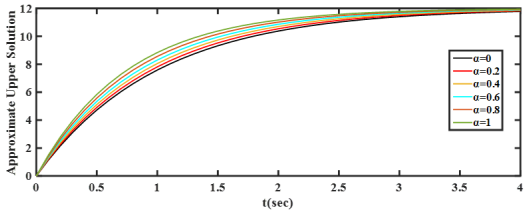

Figure 18. Uncertain Behaviour of the model 5 using OIS with Charging Upper Bound

seen according to Figures 17 and 18 that the solution (membership values with α-cuts) of the charging capacitor model in Equation (26) decreases with the lower bound and increases with the upper bound with the time interval $[0, 4]$. In addition, the use of the triangular fuzzy number for the initial condition of the capacitor charging model was a range of $[2, 4]$ for time t. This gives more information for the approximate solution $\tilde{u}(x)$ of the model such that over initial condition $\tilde{u}(0) = (2,\ 3,\ 4)$, $\tilde{u}(x) = (11.996,\ 11.942,\ 11.780)$ correspondingly. Capacitor is fully

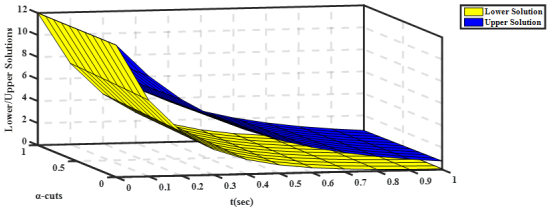

Figure 19. The 3-Dimensional solution via developed OIS for model 5 with Discharging for all $t, \alpha \in [0, 1]$.

discharged when the uncertain parameter $\alpha = 0$ and it is also seen according to Figures 20 and 21 that the solution

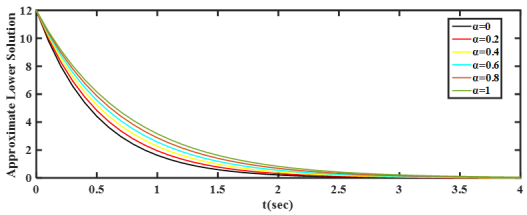

Figure 20. Uncertain Behaviour of the model 5 using OIS with Discharging Lower Bound

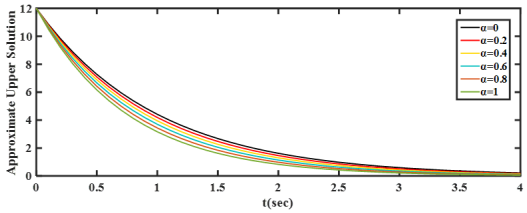

Figure 21. Uncertain Behaviour of the model 5 using OIS with Discharging Upper Bound

(membership values with α-cuts) of the discharging capacitor model in Equation (26) increases with the lower bound and decreases with the upper bound with the time interval $[0, 4]$. In addition, the use of the triangular fuzzy number for the initial condition of the capacitor discharging model was a range of $[2, 4]$ for time . This gives more information for the approximate solution $\tilde{u}(t)$ of the model such that over initial condition $\tilde{u}(0) = (2,\ 3,\ 4)$, $\tilde{u}(t) = (0.004,\ 0.057,\ 0.219)$ correspondingly.

5. Conclusion

The primary goal of this study was to develop a numerical technique for solving first-order FDEs with improved accuracy in terms of the absolute error of the solutions. To solve these FDEs, this research took into consideration the development of OISs with the presence of two higher derivatives. The numerical results obtained also display the superior accuracy of the OIS. Hence, the primary goal of the study was achieved. This research is to develop OIS with two higher derivative terms using the Taylor series approach for solving first-order FDEs. The findings led to the conclusion that the OIS developed in this study with the presence of two higher derivative terms are zero-stable, absolutely stable, and also satisfy the theoretical properties for linear multistep methods to ensure convergence. This research was to apply the constructed method to real-life problems. In different models were solved by the developed OIS in this study. This constructed method successfully solved these real-life models with improved accuracy in terms of absolute error. The benefit of considering models in fuzzy form is that the initial circumstances are thought to be precisely described within a model, which makes it easier to analyse the uncertain behaviour of these models. Hence the methods developed in this study are viable approaches for solving FDEs.

Acknowledgement

We thank the referees for the positive and enlightening comments and suggestions that have greatly helped us to improve this paper.

REFERENCES

1. Hussain, K., Amourah, A., Salah, J., Jameel, A. F., and Anakira, N, *(2025). Autonomous block method for uncertainty analysis in first-order real-world models using fuzzy initial value problem*, AIMS MATHEMATICS, vol,10, no.4, pp. 9614-9636, 2025
2. Akram, M., and Bilal, M. *Analytical solution of bipolar fuzzy heat equation using homotopy perturbation method*, Granular Computing, vol. 8, no. 6, pp. 1253-1266, 2023.
3. Puri, M. L., and Ralescu, D. A. *Differentials of fuzzy functions*, Journal of Mathematical Analysis and Applications, vol. 91, no. 2, pp.552-558, 1983.
4. Seikkala, S. *(1987). On the fuzzy initial value problem*, Fuzzy Sets and Systems, vol. 24, no. 3, pp. 319-330, 1987.
5. Bede, B., and Stefanini, L. *Generalized differentiability of fuzzy-valued functions*, Fuzzy Sets and Systems, vol. 230, pp. 119-141, 2013.
6. Ma, M., Friedman, M., and Kandel, A. *Numerical solutions of fuzzy differential equations*, Fuzzy Sets and Systems, vol. 105, no. 1, pp. 133-138, 1999.
7. Shokri, J. *Numerical solution of fuzzy differential equations*, Applied Mathematical Sciences, vol. 45, no. 1, pp. 2231-2246, 2007.
8. Najafi, H. S., Sasemasi, F. R., Roudkoli, S. S., and Nodehi, S. F. *Comparison of two methods for solving fuzzy differential equations based on Euler method and Zadeh?s extension*, The Journal of Mathematics and Computer Science, vol. 2, no. 2, pp. 295-306, 2011.
9. Jayakumar, T., and Kanakarajan, K. *Numerical solution for hybrid fuzzy system by improved Euler method*, International Journal of Applied Mathematical Science, vol. 6, no. 38, pp. 1847-1862, 2012.
10. Smita, T., and Chakraverty, S. *Euler-based new solution method for fuzzy initial value problems*, International Journal of Artificial Intelligence and Soft Computing, vol.4, no. 1, pp. 58-79, 2014
11. Sevindir, K., and Cetinkaya, H. *On numerical solutions of fuzzy differential equations*, International Journal of Development Research, vol. 8, no. 09, pp. 22971-22979, 2018.
12. Ahmady, N., Allahviranloo, T., and Ahmady, E. *A modified Euler method for solving fuzzy differential equations under generalized differentiability*, Computational and Applied Mathematics, vol. 39, no. 2, pp. 1-21, 2020
13. Omole, E. O., Adeyefa, E. O., Ayodele, V. I., Shokri, A., and Wang, Y. *Ninth-order multistep collocation formulas for solving models of pdes arising in fluid dynamics*, Design and implementation strategies. Axioms, vol. 12, no. 9, pp. 891, 2023.
14. Allahviranloo, T., Abbasbandy, S., Ahmady, N., and Ahmady, E. *Improved predictor-corrector method for solving fuzzy initial value problems*, Information Sciences, vol. 179, no. 7, pp. 945-955, 2009.
15. Prakash, P., and Kalaiselvi, V. *Numerical solutions of fuzzy differential equations by using hybrid methods*, Fuzzy Information and Engineering, vol. 4, no. 4, pp. 445-455, 2012.
16. Salih, M. M. *Using Predictor-Corrector methods for solving fuzzy differential equations*, Discovering Mathematics (Menemui Matematik), vol. 36, no. 1, pp. 9-17, 2014.
17. Ivaz, K., Khastan, A., and Nieto, J. J. *A numerical method for fuzzy differential equations and hybrid fuzzy differential equations*, Abstract and Applied Analysis Hindawi . vol. 2013, no. 3, pp. 1-10, 2013.
18. Ahmad, N. B., Kavikumar, J., Mamat, M., Hamzah, A., and Shamsidah, N. *Fuzzy differential equations by using modified Romberg's method*, Prosiding Seminar Kebangsaan Aplikasi Sains dan Matematik vol. 29, no. 2013, pp. 51-64, 2013.
19. Maghool, F. H., Radhy, Z. H., Mehdi, H. A., and Abass, H. M. *Simpson's rule to solve fuzzy differential equations*, International Journal of Advanced Research in Science, Engineering and Technology. vol. 6, no. 10, pp. 11306-11315, 2019 .
20. Abbasbandy, S., Viranloo, T. A., Lopez-Pouso, O., and Nieto, J. J. *Numerical methods for fuzzy differential inclusions*, Computers & Mathematics with Applications, vol. 48, no. 10, pp. 1633-1641, 2004.
21. Ibrahim, I., Taha, W., Dawi, M., Jameel, A., Tashtoush, M., Az-Zo?bi, E. *Various Closed-Form Solitonic Wave Solutions of Conformable Higher-Dimensional Fokas Model in Fluids and Plasma Physics*, Iraqi Journal For Computer Science and Mathematics, vol. 5, no. 3, pp. 401-417, 2024.
22. Jameel, A. F., Ismail, A. I. M., and Sadeghi, A. *Numerical solution of fuzzy IVP with trapezoidal and triangular fuzzy numbers by using the fifth-order Runge-Kutta method*, World Applied Sciences Journal, 17(12), 1667-1674.
23. Parandin, N. *Numerical solution of fuzzy differential equations of 2nd-order by Runge-Kutta method*, Journal of Mathematical Extension, vol. 7, no. 3, pp. 47-62, 2014.
24. Nirmala, V., Parimala, V., and Rajarajeswari, P. *Application of Runge-Kutta method for finding multiple numerical solutions to intuitionistic fuzzy differential equations*, In Journal of Physics: Conference Series vol. 1139 no. 1, pp. 1-8, 2018.
25. Ahmadian, A., Salahshour, S., Chan, C. S., and Baleanu, D. *Numerical solutions of fuzzy differential equations by an efficient Runge?Kutta method with generalized differentiability*, Fuzzy Sets and Systems, vol. 33, no. 1, pp. 47-67, 2018.
26. Mehrkanoon, S., Suleiman, M., and Majid, Z. *Block method for numerical solution of fuzzy differential equations*, International Mathematical Forum, vol. 4, no. 6, pp. 2269 - 2280, 2009.
27. Zawawi, I. S., Ibrahim, Z. B., and Suleiman, M. *Diagonally implicit block backward differentiation formulas for solving fuzzy differential equations*, AIP Conference Proceedings, vol. 1522, no. 1, pp. 681-687, 2013.
28. Ramli, A., and Majid, Z. A. *Fourth-order diagonally implicit multistep block method for solving fuzzy differential equations*, International Journal of Pure and Applied Mathematics, vol. 107, no. 3, pp. 635-660, 2016.
29. Fook, T. K., and Ibrahim, Z. B. *Two points hybrid block method for solving first-order fuzzy differential equations*, Journal of Soft Computing Applications, vol. 20, no. 1, pp. 45-53, 2016.
30. Ramli, A., and Majid, Z. A. *An implicit multistep block method for fuzzy differential equations*, International Conference On Research And Educations In Mathematics (ICREM7) vol. 107, no. 3, pp. 113-119, 2015.
31. Isa, S., Abdul Majid, Z., Ismail, F., and Rabiei, F. *Diagonally implicit multistep block method of order four for solving fuzzy differential equations using Seikkala derivatives*, Symmetry, vol. 10, no. 2, pp. 42-63, 2018 .
32. Jameel, A. F., Anakira, N. R., Alomari, A., Alsharo, D., and Saaban, A. *New semi-analytical method for solving two-point nth order fuzzy boundary value problem*, International Journal of Mathematical Modelling and Numerical Optimisation, vol. 9, no. 1, pp. 12-31, 2019.

33. Hussain K, Adeyeye O, and Ahmad N. *Higher Derivative Block Method with Generalised Steplength for Solving First-Order Fuzzy Initial Value Problems*, IIUM Eng J. vol. 24, no. 1, pp. 158-169, 2023.
34. Hussain, K., Adeyeye, O., and Ahmad, N. *Numerical Solution of Second Order Fuzzy Ordinary Differential Equations using Two-Step Block Method with Third and Fourth Derivatives*, Journal of the Nigerian Society of Physical Sciences, vol. 5, no. 1, pp. 1087-1087, 2023.
35. Hussain, K., Adeyeye, O., Ahmad, N., & Bibi R. *Third-Fourth Derivative Three-Step Block Method for Direct Solution of Second-Order Fuzzy Ordinary Differential Equations*, IAENG Int J Comput Sci. vol. 49, no. 3, pp. 856-863, 2022.
36. Jafari, R., Yu, W., Li, X., & Razvarz, S. *Numerical solution of fuzzy differential equations with Z-numbers using Bernstein neural networks*, International Journal of Computational Intelligence Systems, vol. 10, no. 1, pp. 1226-1237, 2017.
37. Saadoon, N., Abduirazzaq, N., Hussain, A., Mohammed, N., Az-Zo?bi, E., Tashtoush, M. *Numerical Solutions for Fuzzy Stochastic Ordinary Differential Equations Using Heun?s Method with a Dual-Wiener Process Framework*, Mathematical Modelling of Engineering Problems, vol. 12, no. 3, pp. 763-773, 2025.
38. Az-Zo?bi, E., Kallekh, A., Rahman, R., Akinyemi, L. Bekir, A., Ahmad, H., Tashtoush, M., Mahariq, I. *Novel topological, non-topological, and more solitons of the generalized cubic p-system describing isothermal flux*, Optical and Quantum Electronics, vol. 56, no. 1, pp. 1-16, 2024.